

Supplementary Figures

Figure S1. The difference of ctDNA properties in patients with different clinical characteristics and distinct histological subtypes.

Figure S2. Number of SNVs/Indels in blood and ctDNA level demonstrate significantly linear dependence in different histological subtypes.

Figure S3. Mutational and pathway landscape for the stage IV, untreated population.

Figure S4. Distribution of mutational types for frequently altered genes in different histological subtypes.

Figure S5. Percentage of pathway alterations in each sample.

Figure S6. Pathway members and interactions in the 10 selected pathways.

Figure S7. Samples with different *EGFR* driver mutations show little discrepancy about ctDNA properties and patient prognosis.

Figure S8. *EGFR* clonality and concurrent *TP53* mutation in ctDNA cohort from

stage IV, untreated population.

FigureS9. Concurrent mutant genes for different *EGFR* driver mutations in the stage IV, untreated cohort.

Figure S10. The ctDNA properties and pathway alterations in the stage IV, untreated, NSCLC subset with *RBI* mutations.

Figure S11. The interaction between somatic mutational events in the stage IV, untreated, NSCLC subset with *RBI* mutations.

Figure S12. Genomic concordance between paired tissue and blood samples.

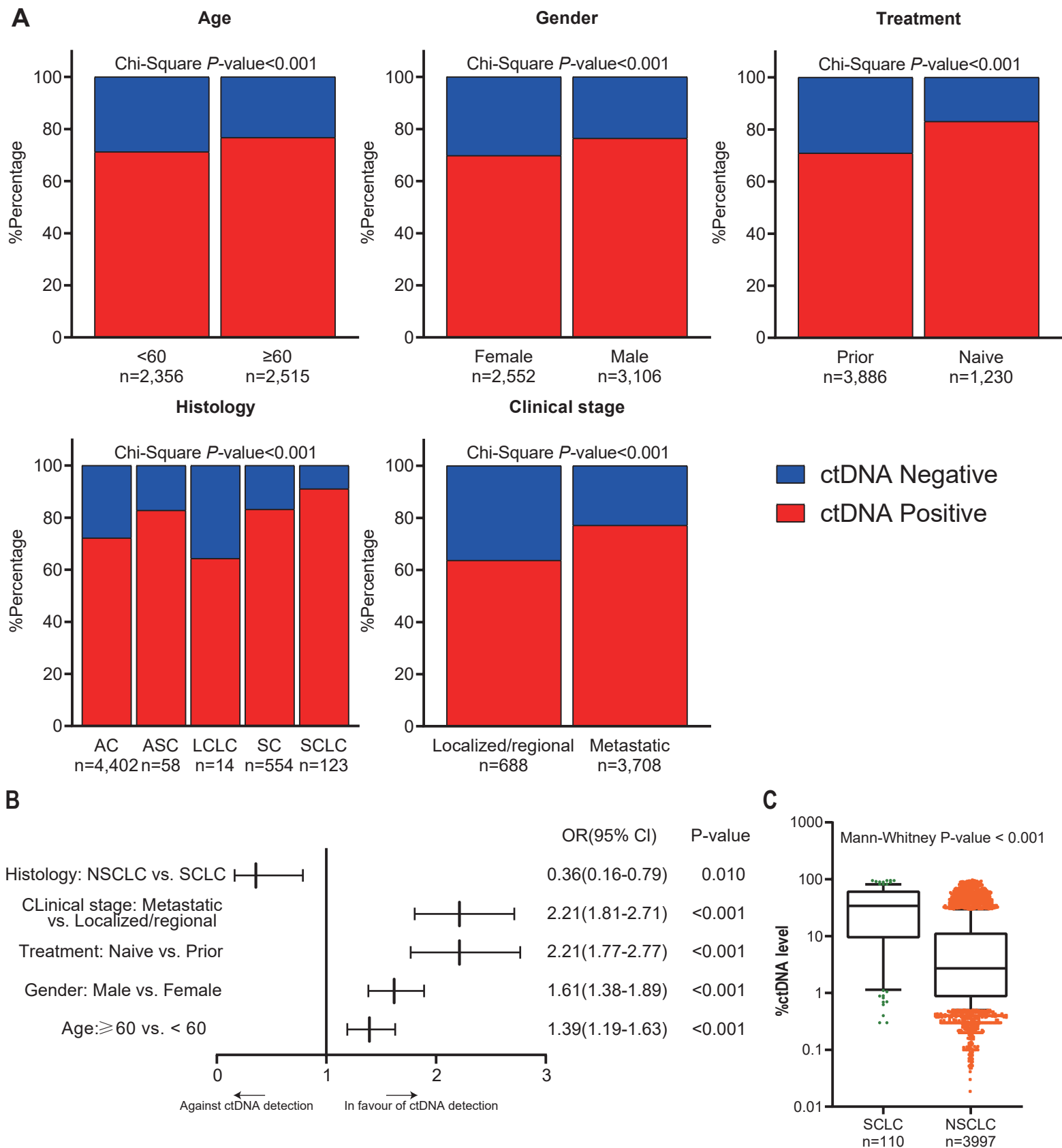


Figure S1. The difference of ctDNA properties in patients with different clinical characteristics and distinct histological subtypes. (A) ctDNA detectability varies in patients with different clinical characteristics. AC, adenocarcinoma; ASC, adenosquamous carcinoma; LCLC, large cell lung cancer; SC, squamous carcinoma; SCLC, small cell lung cancer. (B) Forest plot shows clinical factors and histological subtypes significantly influencing ctDNA detectability. Statistics is performed using Binary Logistic Regression and corresponding parameters are listed in the right part of the panel. NSCLC, non-small cell lung cancer. (C) ctDNA level fluctuate obviously between NSCLC and SCLC. P -value < 0.05 is identified as statistical significance.

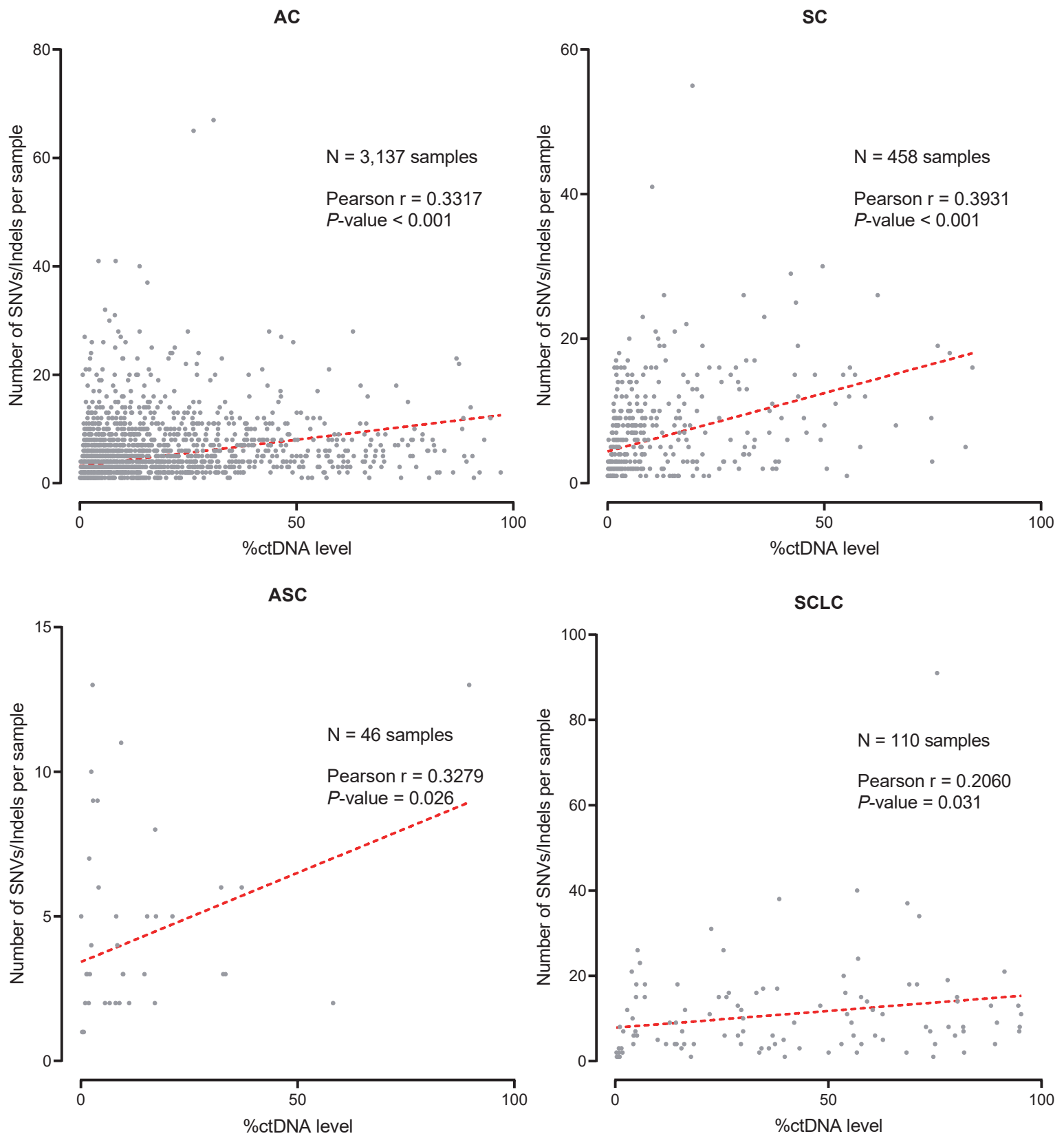


Figure S2. Number of SNVs/Indels in blood and ctDNA level demonstrate significantly linear dependence in different histological subtypes. ctDNA level indicates the maximal variant AF in each blood sample. Pearson's coefficient is used to evaluate the correlation and P -value < 0.05 is identified as statistical significance.

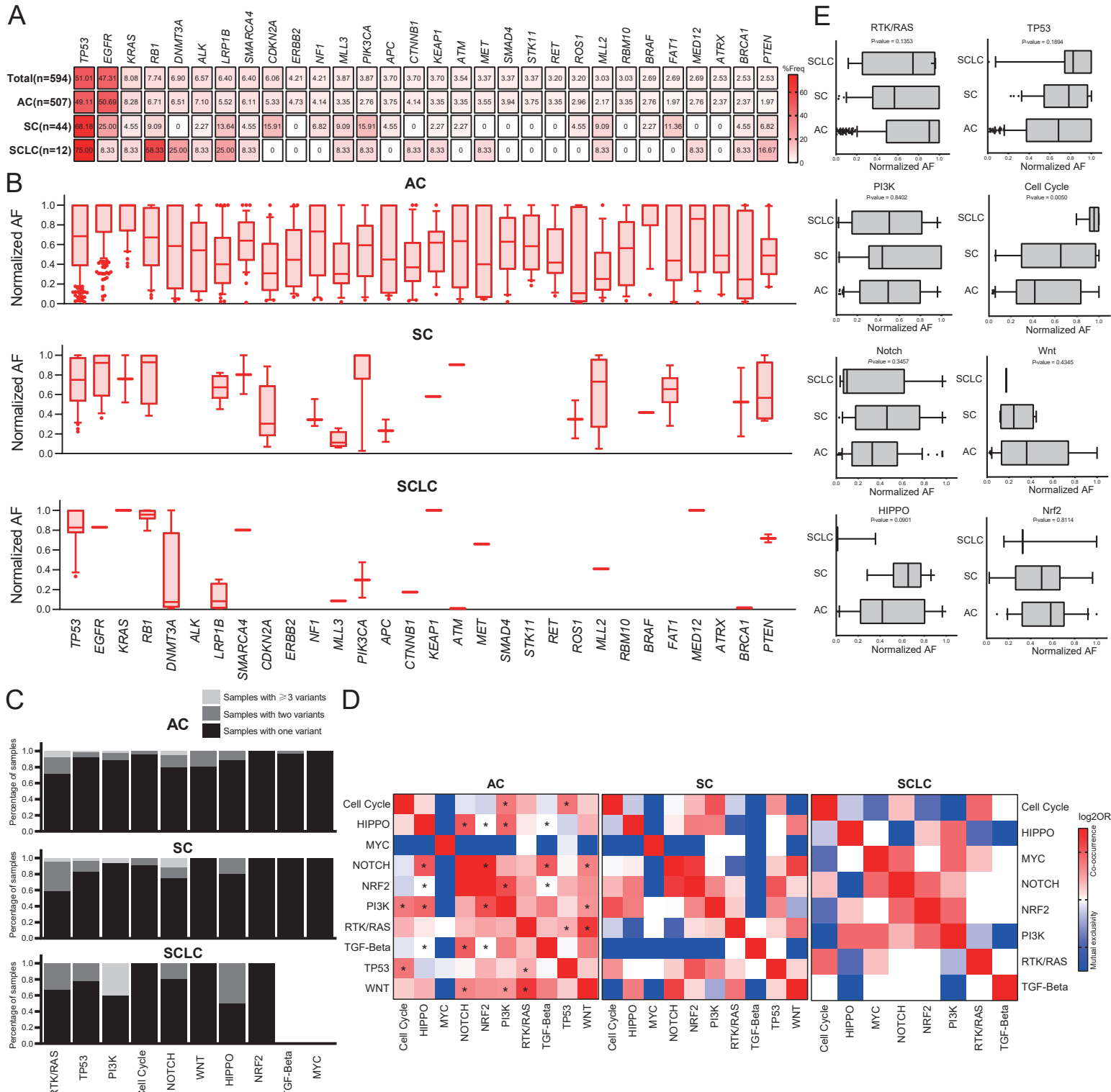


Figure S3. Mutational and pathway landscape for the stage IV, untreated population. (A) Frequently altered gene in this cohort and different subtypes. Color gradation indicates the prevalence of each mutant gene. AC, adenocarcinoma; SC, squamous carcinoma; SCLC, small cell lung cancer. (B) Box plots illustrate the normalized AF of different mutant genes in AC, SC, and SCLC. Centre line, median; box limits, upper and lower quartiles; whiskers, 10%-90% data range. (C) Percentage of samples harboring specific numbers of variant within the same pathways. (D) Mutual exclusivity (blue) and co-occurrence (red) among pathway alterations. The co-occurrence and mutual exclusivity of one pathway (assumed as A) with another pathway (assumed as B) was estimated via odds ratio (OR) and q-value derived from Benjamini-Hochberg FDR correction procedure. $OR = \frac{\text{Neither} * \text{Both}}{\text{A Not B} * \text{B Not A}}$. Those pathway pairs with $OR > 4$ or < 0.25 and $q\text{-value} < 0.05$ are identified as significantly enriched co-pathways or mutually exclusive pathways which are labelled with asterisks. (E) Normalized AFs of pathway alterations vary among different AC, SC, and SCLC. Centre line, median; box limits, upper and lower quartiles; whiskers, 10%-90% data range. Statistics is performed using One-way ANOVA and P-value < 0.05 is identified as statistical significance.

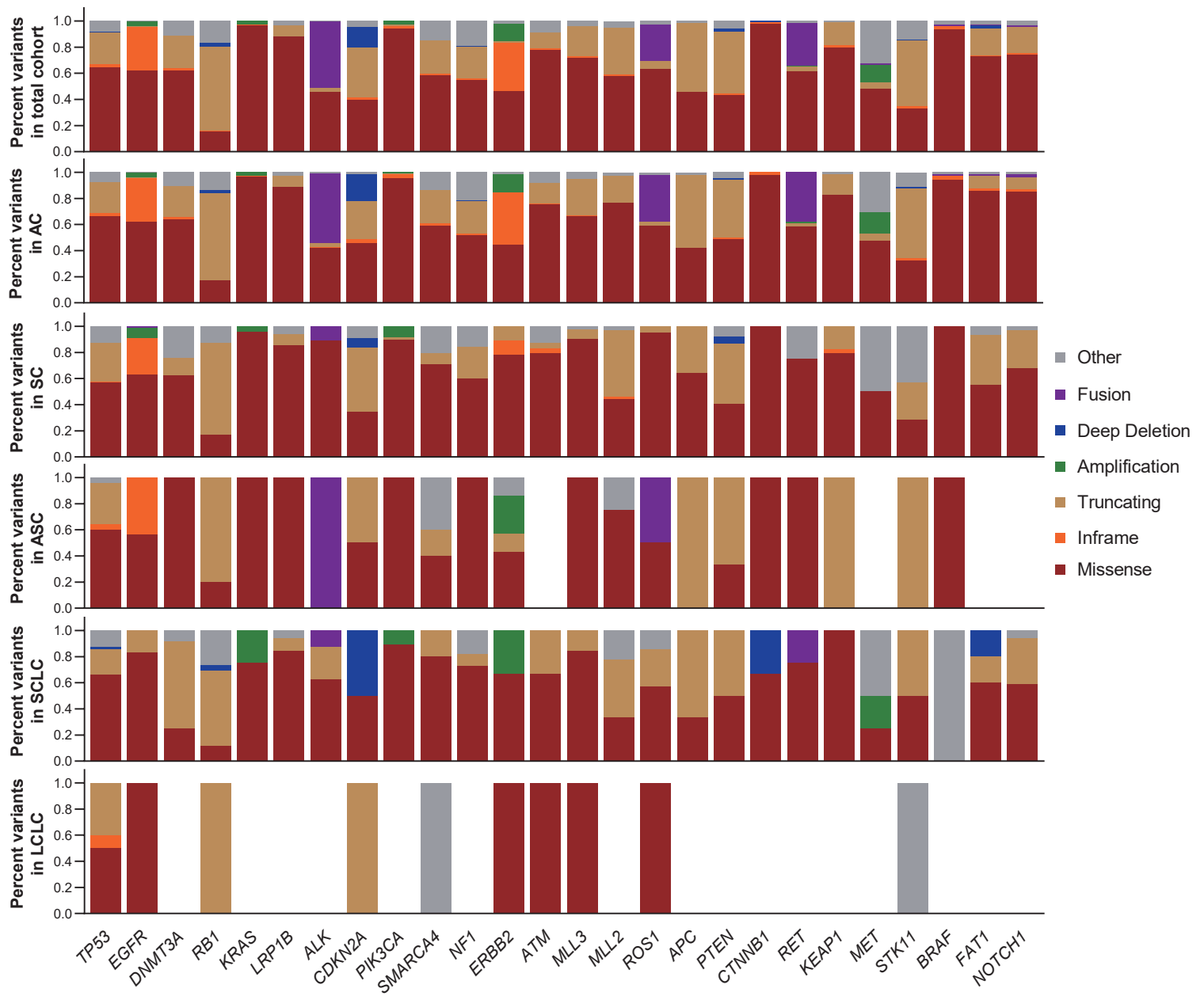


Figure S4. Distribution of mutational types for frequently altered genes in different histological subtypes. Top 26 genes in the total cohort are illustrated.

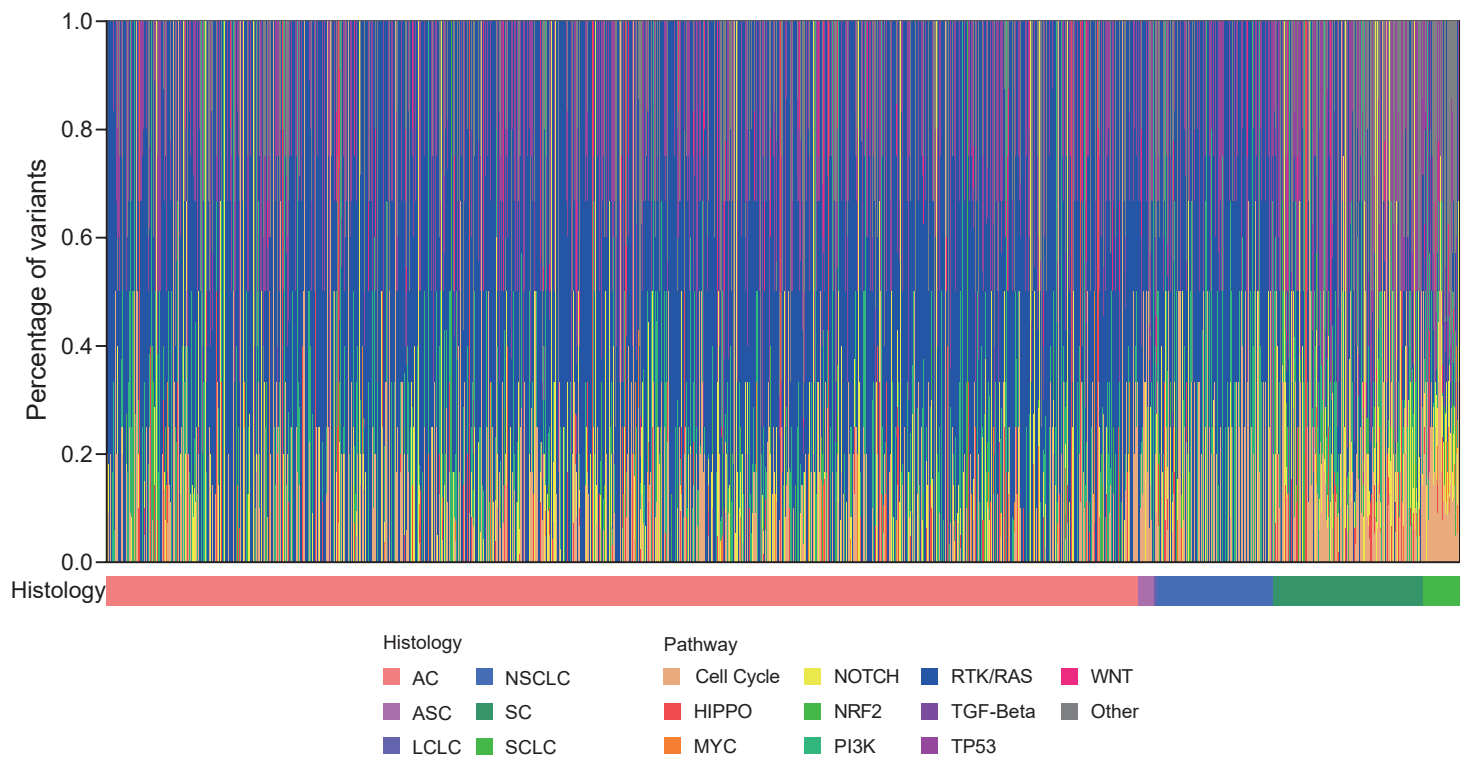


Figure S5. Percentage of pathway alterations in each sample. The histological subtype is displayed below in the chart.

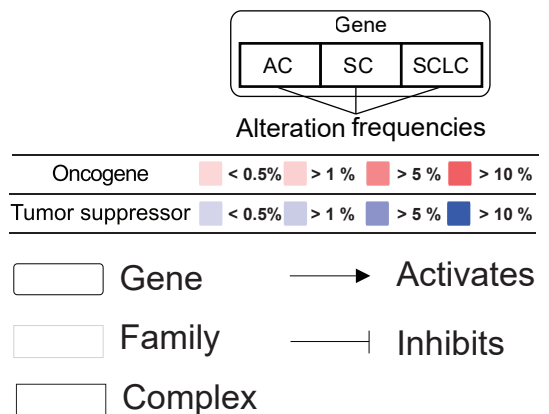
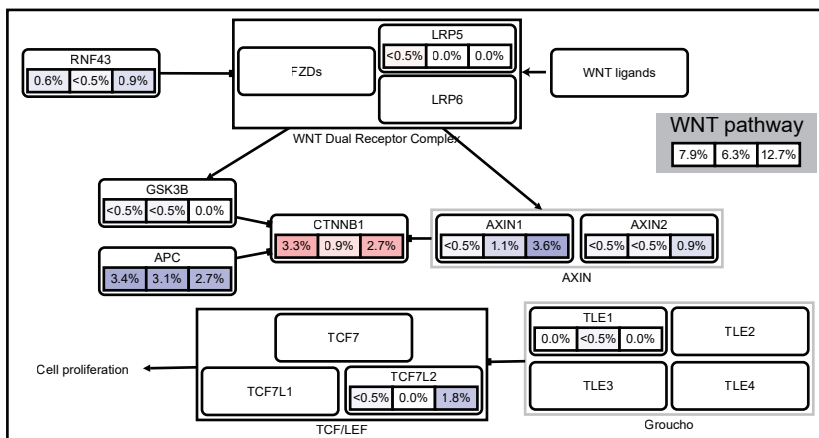
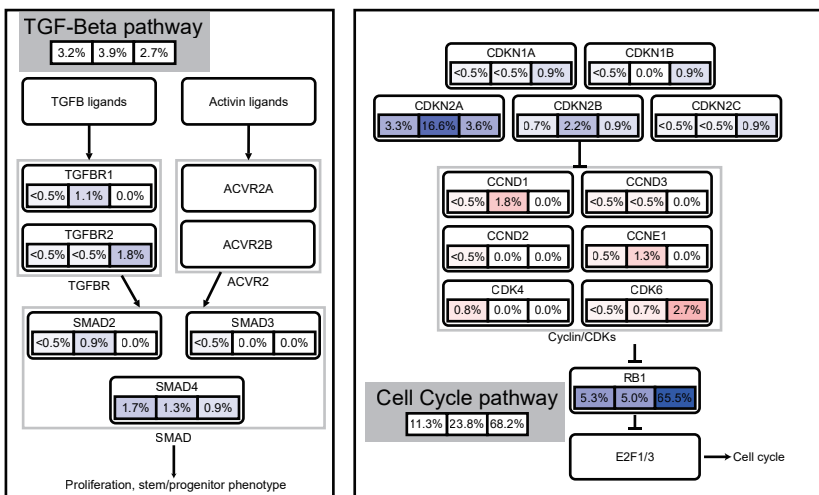
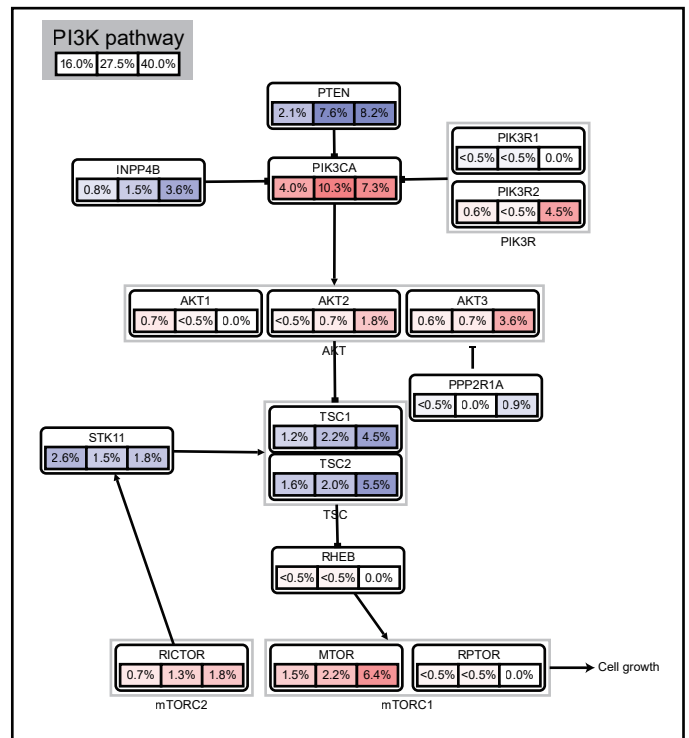
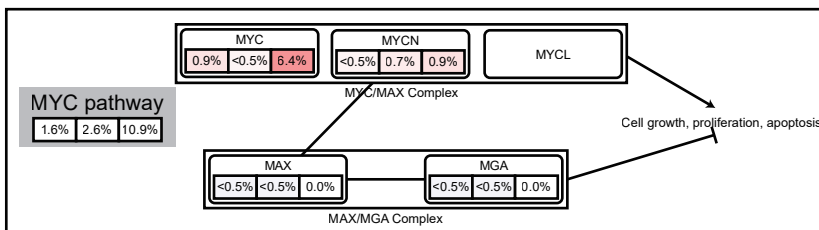
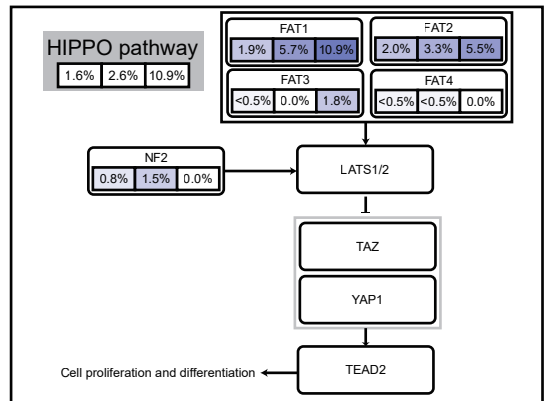
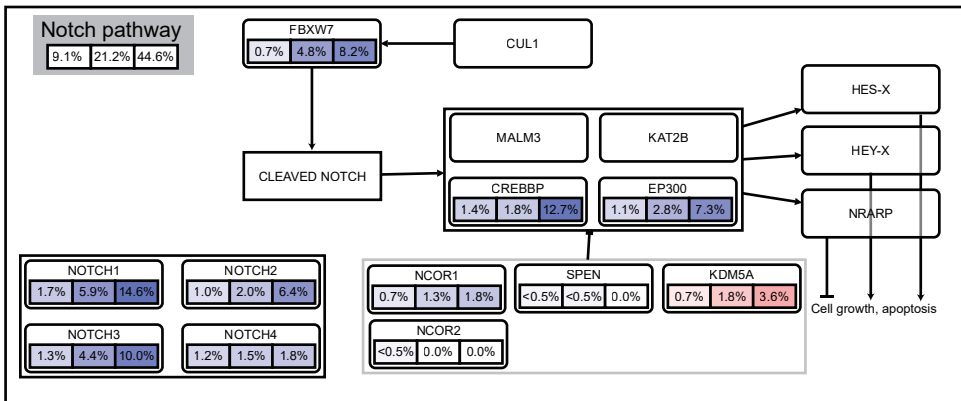
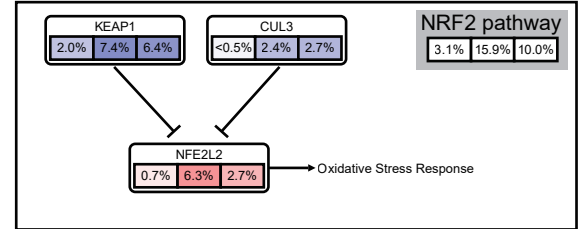
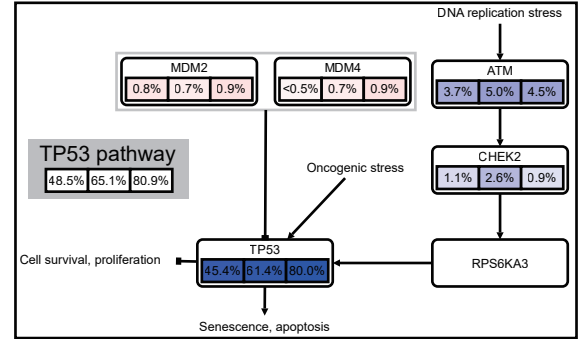
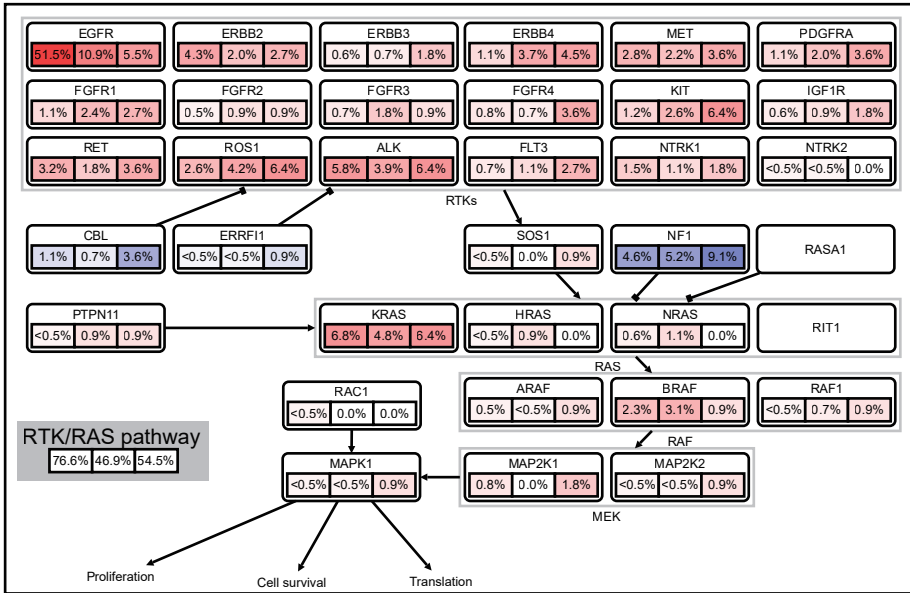


Figure S6. Pathway members and interactions in the 10 selected pathways. Oncogenes and tumor suppressor genes are illustrated with red and blue, respectively. Color intensity indicates the frequency of alteration within the entire dataset. Blank boxes represent genes not covered in our sequencing panel.

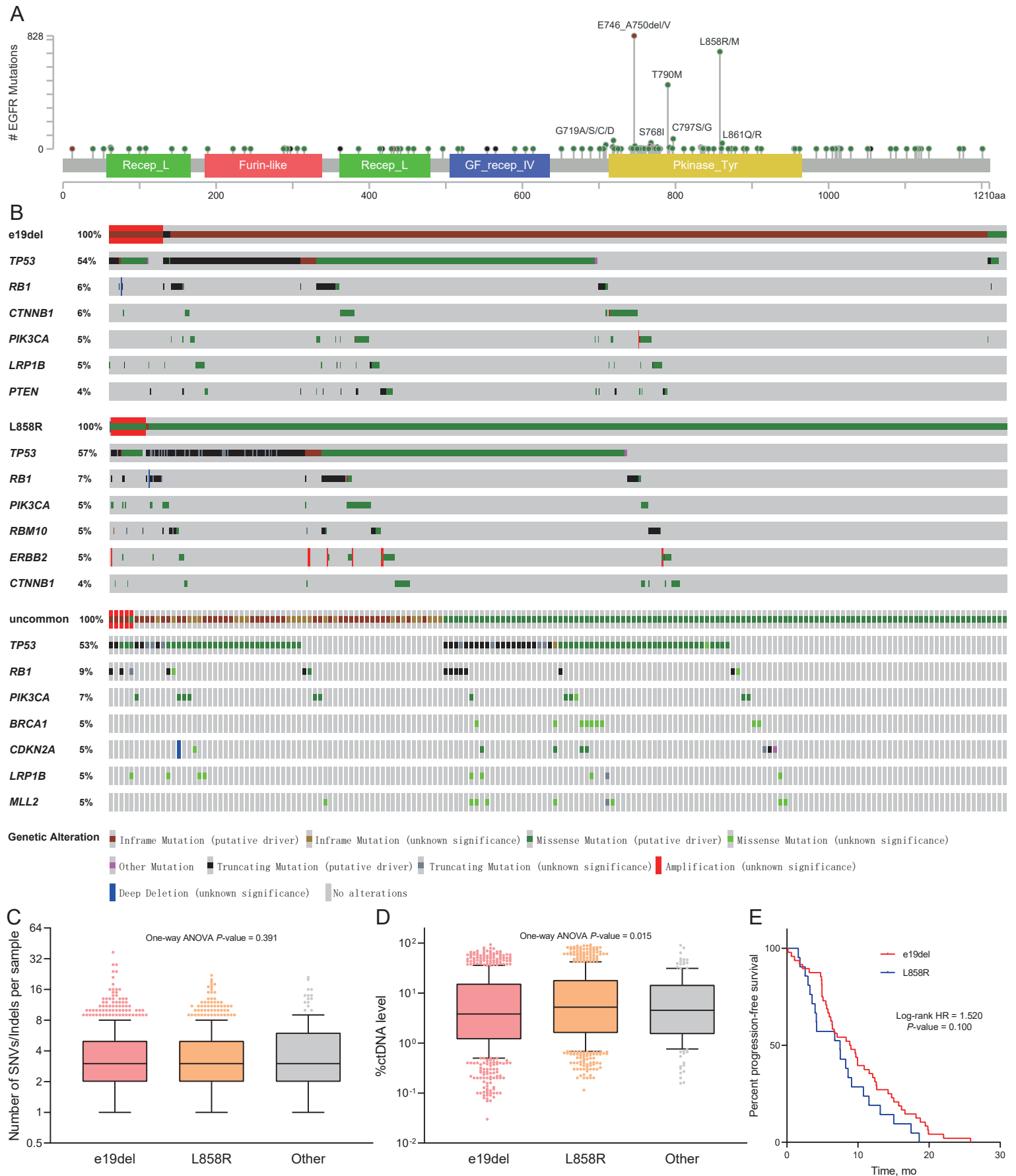


Figure S7. Samples with different *EGFR* driver mutations show little discrepancy about ctDNA properties and patient prognosis. (A) Lollipop chart illustrates the overview of all *EGFR* mutations. (B) Concurrent mutant genes for different *EGFR* driver mutations. (C) The number of SNVs/Indels in blood is similar among subsets with different *EGFR* driver mutations. (D) Samples with *EGFR* L858R show elevated ctDNA level compared with other *EGFR*-mutant samples. (E) Patients with e19del and L858R in blood ctDNA demonstrate similar PFS. Kaplan-Meier survival analysis is used to evaluate prognosis of different subgroups and P -value < 0.05 is identified as statistical significance.

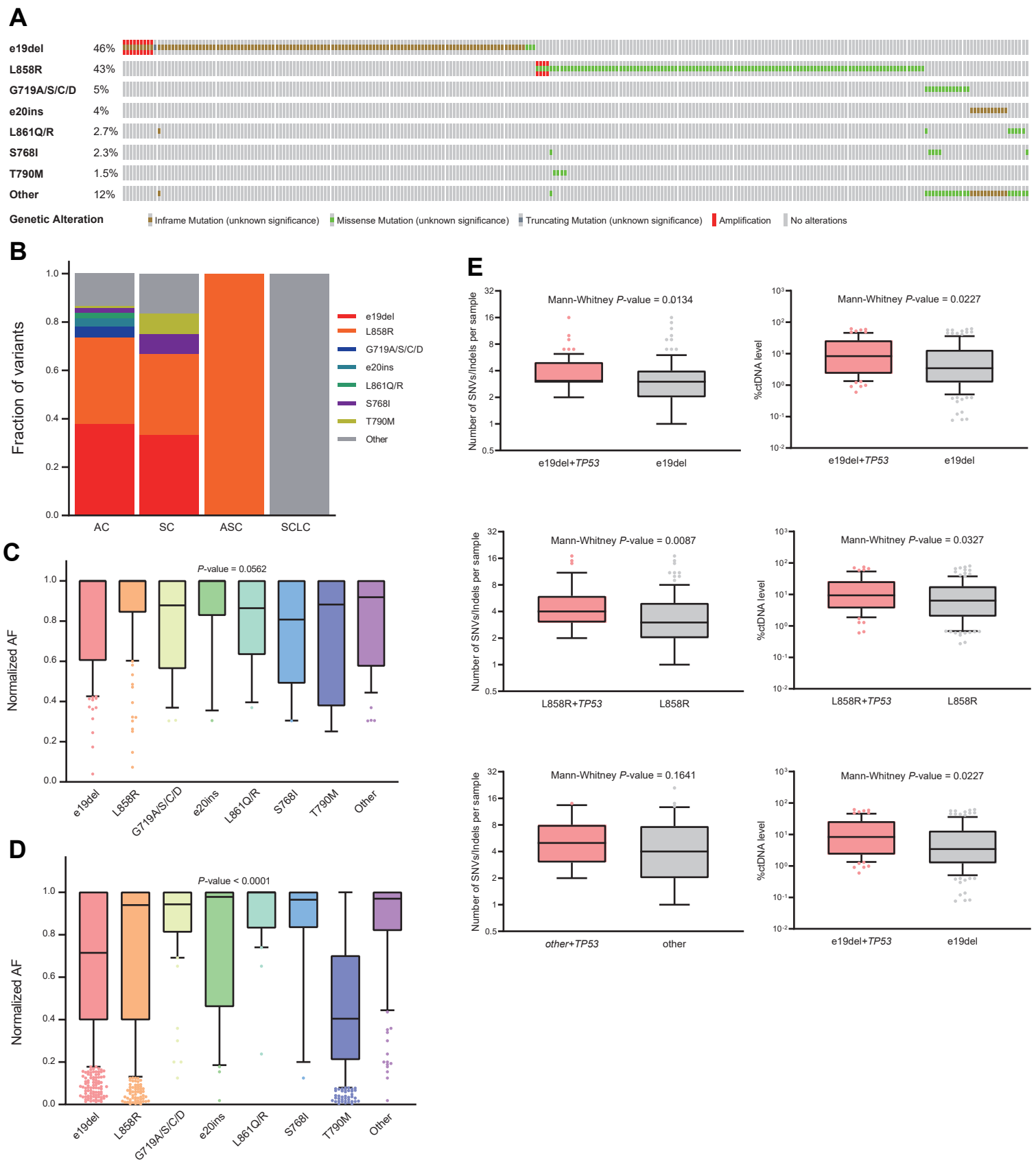


Figure S8. *EGFR* clonality and concurrent *TP53* mutation in ctDNA cohort from stage IV, untreated population. (A) Heatmap shows the presence of different mutation in *EGFR*-mutant samples. e19del, exon 19 deletion; AMP, amplification; e20ins, exon 20 insertion. (B) Distribution of different *EGFR* mutations among diverse *EGFR*-mutant subtypes. AC, adenocarcinoma; SC, squamous carcinoma; ASC, adenosquamous carcinoma; SCLC, small cell lung cancer. (C) and (D) Normalized AFs of different *EGFR* mutations in the stage IV, untreated cohort and the stage IV, treated cohort, respectively. Centre line, median; box limits, upper and lower quartiles; whiskers, 10%-90% data range. Statistics is performed using One-way ANOVA and P-value <0.05 is identified as statistical significance. (E) The number of SNVs/Indels in blood and ctDNA level are increased in samples with concurrent *EGFR* driver events and *TP53* mutations compared with *EGFR*-only samples. Centre line, median; box limits, upper and lower quartiles; whiskers, 10%-90% data range. Statistics is performed using Mann-Whitney U test and P-value <0.05 is identified as statistical significance.



Figure S9. Concurrent mutant genes for different *EGFR* driver mutations in the stage IV, untreated cohort.

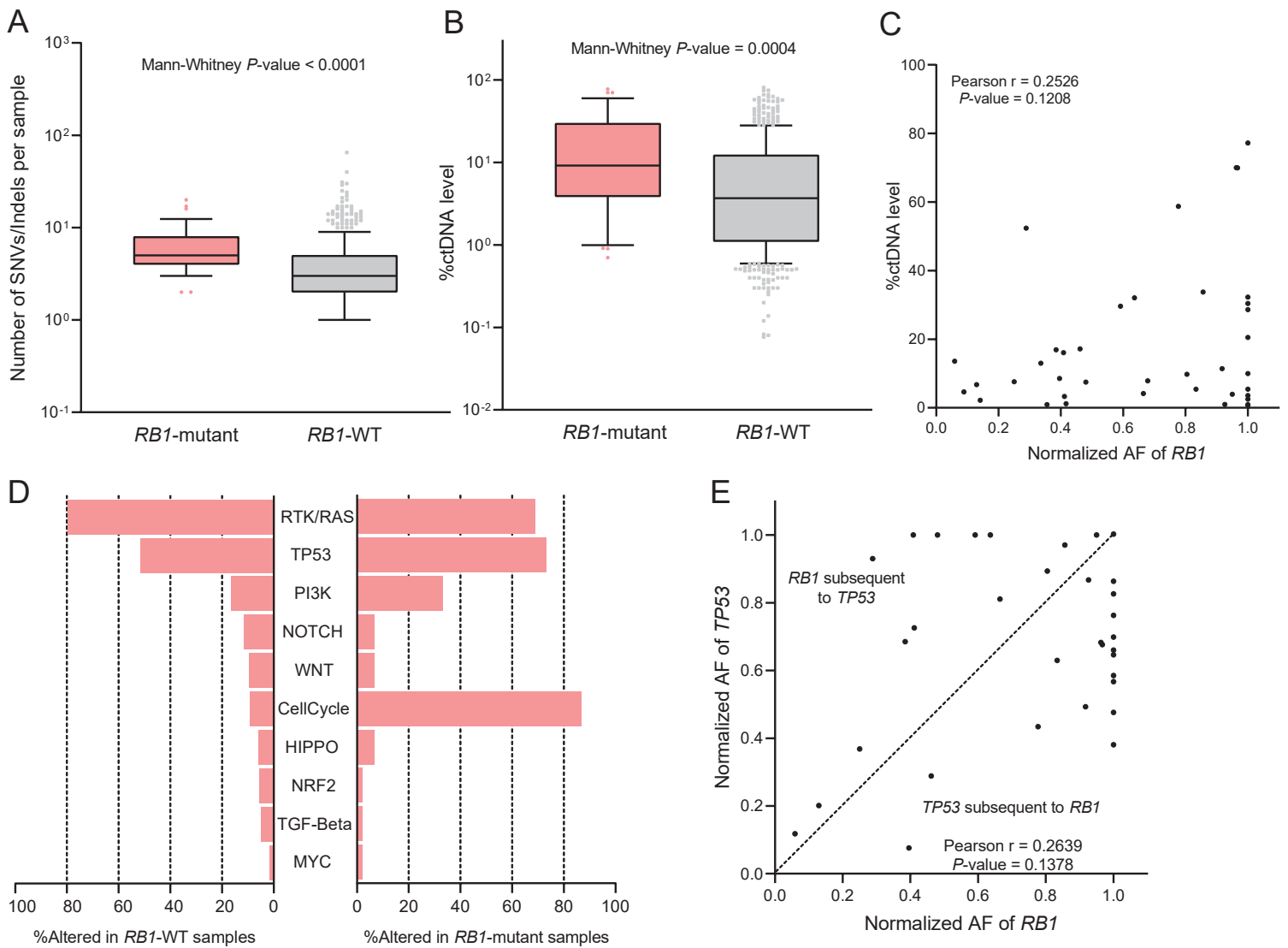


Figure S10. The ctDNA properties and pathway alterations in the stage IV, untreated, NSCLC subset with *RB1* mutations. (A) and (B) *RB1*-mutant NSCLC express superior number of SNVs/Indels and ctDNA level compared with *RB1*-wild type NSCLC. Centre line, median; box limits, upper and lower quartiles; whiskers, 10%-90% data range. Statistics is performed using Mann-Whitney U test and P -value < 0.05 is identified as statistical significance. WT, wild type. (C) The normalized AFs of *RB1* mutations are not significantly correlated with the ctDNA level of corresponding samples. Pearson's coefficient is used to evaluate the correlation and P -value < 0.05 is identified as statistical significance. (D) Frequencies of pathway alterations in *RB1*-mutant and *RB1*-wild type NSCLC. Statistics is performed using Chi-square test and P -value < 0.05 is identified as statistical significance which is labelled with asterisks. (E) Correlation between normalized AFs of concurrent *RB1* and *TP53* mutations. Pearson's coefficient is used to evaluate the correlation and P -value < 0.05 is identified as statistical significance.

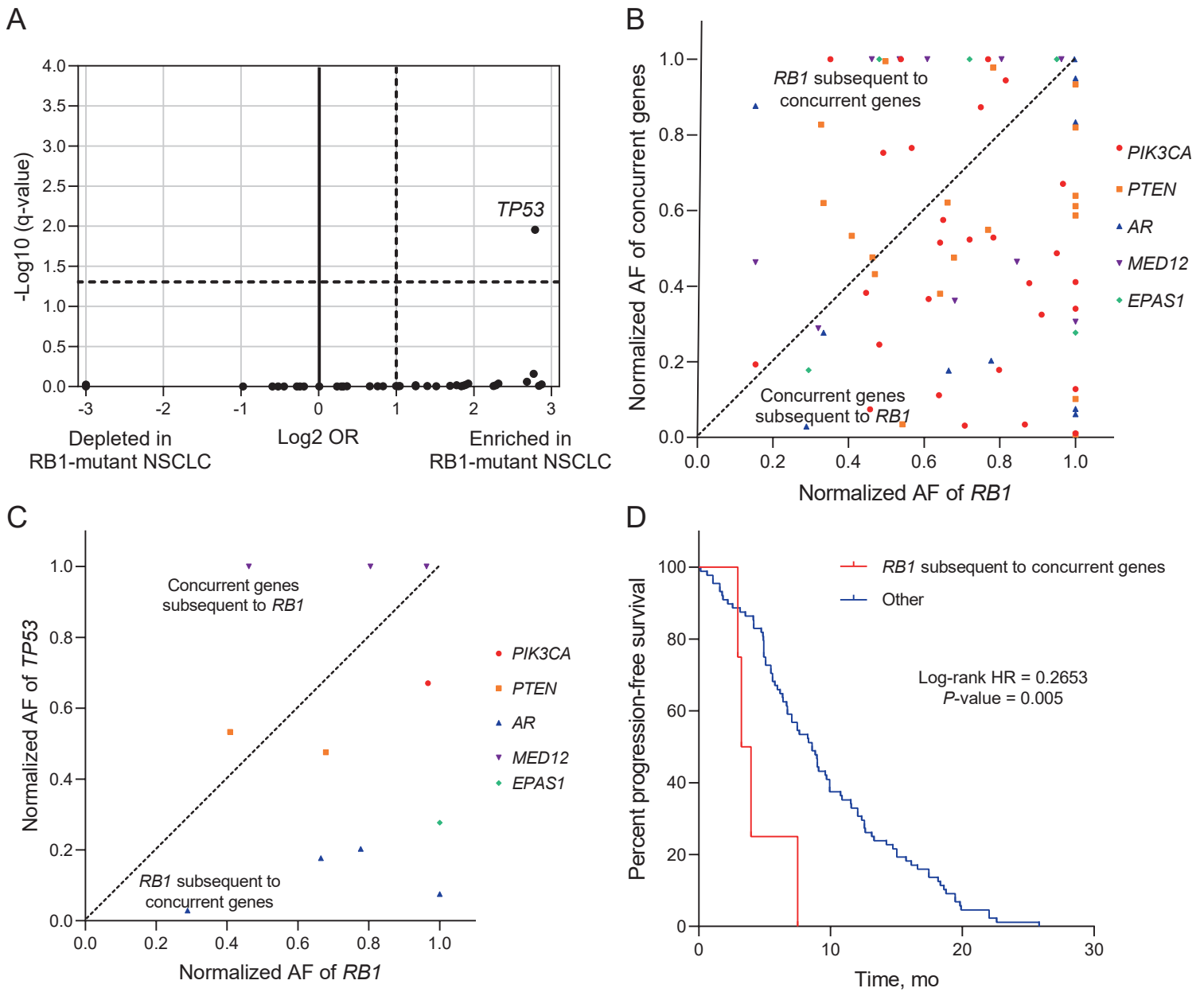


Figure S11. The interaction between somatic mutational events in the stage IV, untreated, NSCLC subset with *RB1* mutations. (A) Mutual exclusivity and co-occurrence among mutant genes. The co-occurrence and mutual exclusivity of one gene (assumed as A) with another gene (assumed as B) was estimated via odds ratio (OR) and q-value derived from Benjamini-Hochberg FDR correction procedure. $OR = \frac{\text{Neither} * \text{Both}}{\text{A Not B} * \text{B Not A}}$. Those gene pairs with $OR > 2$ or < 0.5 and $q\text{-value} < 0.05$ are identified as significantly enriched co-genes or mutually exclusive genes. (B) and (C) Correlation between normalized AFs of concurrent *RB1* and other mutations in NSCLC cohort and the stage IV, untreated NSCLC subset, respectively. (D) PFS is significantly deficient for patients with *RB1* clonality $<$ concurrent genes. Pearson's coefficient is used to evaluate the correlation and $P\text{-value} < 0.05$ is identified as statistical significance. Kaplan-Meier survival analysis is used to evaluate prognosis of different subgroups and $P\text{-value} < 0.05$ is identified as statistical significance.

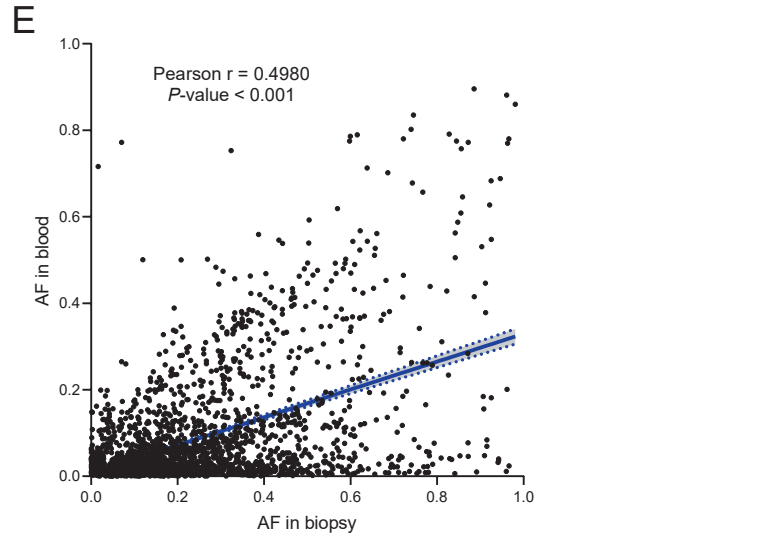
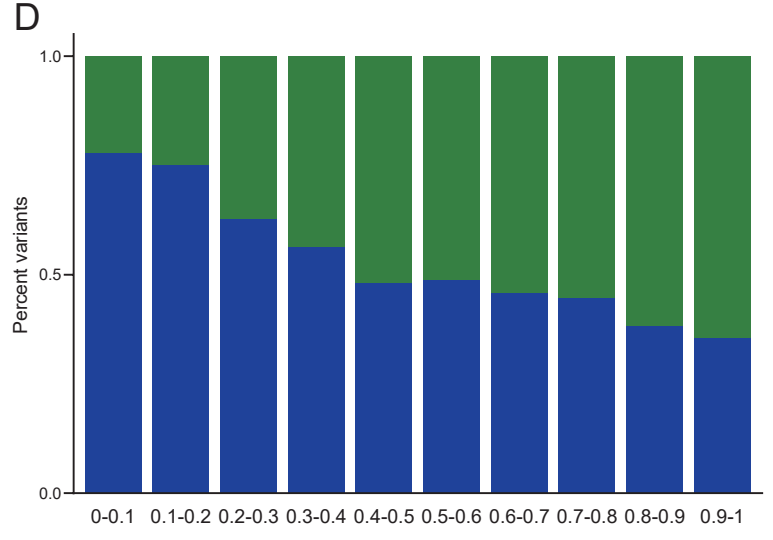
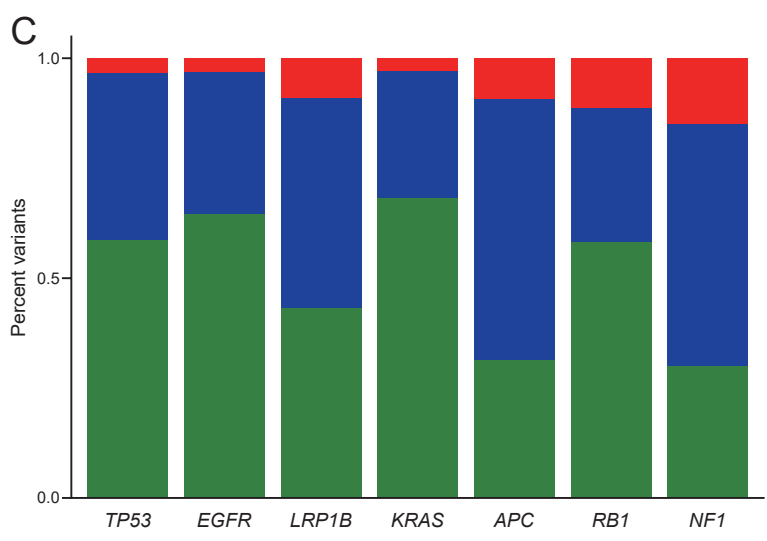
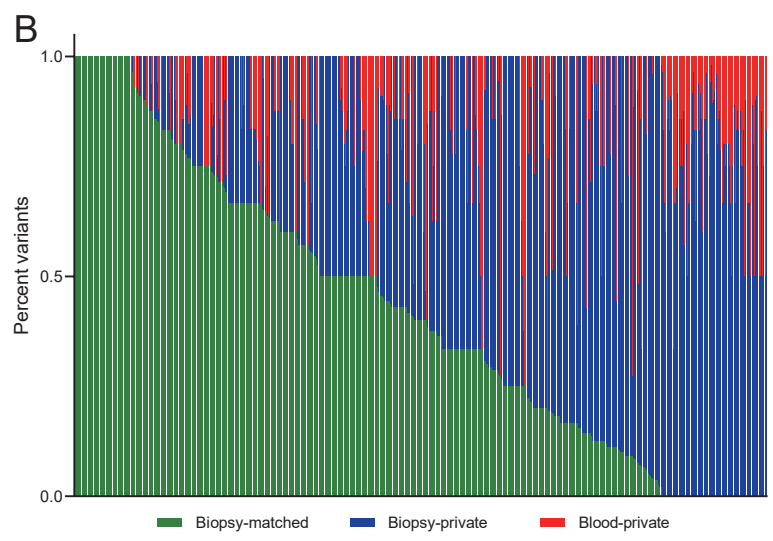


Figure S12. Genomic concordance between paired tissue and blood samples. (A) Genomic landscape of all tissue samples corresponding to blood samples in the primary cohort. (B-D) Distribution of different mutations defined by the presence in paired tissue and blood samples according to patients (B), mutant genes (C), and clonality range of tissue samples (D). (E) AFs of biopsy-matched mutations in paired samples show linear dependence. Pearson's coefficient is used to evaluate the correlation and $P\text{-value} < 0.05$ is identified as statistical significance.